

Electronic Supplementary Information (ESI)

Excitation-Power Responsive Upconversion Logic Operations Based on the Multiphoton Process of Praseodymium Ion

Jingheng Nie,[†] Jianmin Gu,[‡] Weitao Ying,[†] Fei Wang,[§] Shiqing Xu[†] and Shimin Liu^{,†}*

[†]State Key Laboratory of Metastable Materials Science and Technology (MMST), Yanshan
University, Qinhuangdao 066004, China

[‡]Hebei Key Laboratory of Applied Chemistry, School of Environmental and Chemical Engineering,
Yanshan University, Qinhuangdao 066004, China

[§]Faculty of Metallurgical and Energy Engineering, Kunming University of Science and
Technology, Kunming 650093, China

*To whom correspondence should be addressed. E-mail: lsm@ysu.edu.cn.

Experimental

Materials: All of the chemical reagents used in this experiment are analytical grade and were received without further purification. Deionized water was used throughout. Y_2O_3 , Yb_2O_3 , Nd_2O_3 , Pr_2O_3 and EDTA-2Na were purchased from Aladdin Reagent (Shanghai, China). NH_4HF_2 , NaF were provided by Tianjin Kaitong Chemical Reagent Co. Ltd (China).

Calculation: First-principles calculations were based on plane-wave pseudopotential DFT and performed with the CASTEP code. The properties of crystal materials predicted by the CASTEP code involve three steps: model construction, structural optimization and property calculation. Local charge density approximation was applied to describe the exchange correlation energy of electrons. For the optimized geometric calculation, the convergence criteria were as follows: total energy of 5.0×10^{-6} eV/atom, maximum force of 0.01 eV/Å, maximum stress of 0.02 GPa, and maximum displacement of 5.0×10^{-4} Å. A plane-wave cutoff energy of 500 eV was utilized, and a $2 \times 2 \times 4$ k-point mesh was generated in accordance with Monkhorst–Pack. The valence electron configurations of F, Na, Y, and Pr are $2s^22p^5$, $2s^22p^63s^1$, $4s^24p^64d^15s^2$, and $4f^35s^25p^66s^2$, respectively.

Preparation: Hydrothermal method was used for the preparation of NaYF_4 , NaYF_4 : 2 mol% Pr^{3+} , NaYF_4 : 2 mol% Pr^{3+} / 2 mol% Nd^{3+} , and NaYF_4 : 2 mol% Pr^{3+} /15 mol% Yb^{3+} microrods. Rare earth oxides were used as sources of rare earth ions. In a typical experiment, the rare earth oxides were dissolved in nitric acid under heating. EDTA-2Na was added to this solution as a

chelating agent for rare earth ions with magnetic stirring. After 30 min of stirring, NaF and NH_4HF_2 were slowly dropped into the prepared solution, which was stirred for another 30 min. The pH of the solution was adjusted to 6 with $\text{NH}_3 \cdot \text{H}_2\text{O}$, and the solution was transferred to a PTFE-lined high-pressure pot incubated in an oven at 180 °C for 36 h. As the autoclave naturally cooled to room temperature, precipitates were separated through centrifugation, sequentially washed with deionized water and ethanol, and dried at 60 °C for 12 h.

Measurements: X-ray diffraction (XRD) analysis was carried out by using a powder diffractometer (Model D/MAX-2500PC) with Ni-filtered $\text{CuK}\alpha$ radiation ($\lambda = 1.541 \text{ \AA}$) to identify the crystallization phase. Size and morphological characteristics were determined with a scanning electron microscope (SEM, S-3400N II). Emission spectra and fluorescence lifetime were obtained using a Jobin Yvon Fluorolog-3 fluorescence spectrometer system upon 980 nm continuous wave or pulse laser excitations. The same experimental conditions were maintained to obtain the spectra of each group and achieve comparable results. All of the measurements were performed at room temperature.

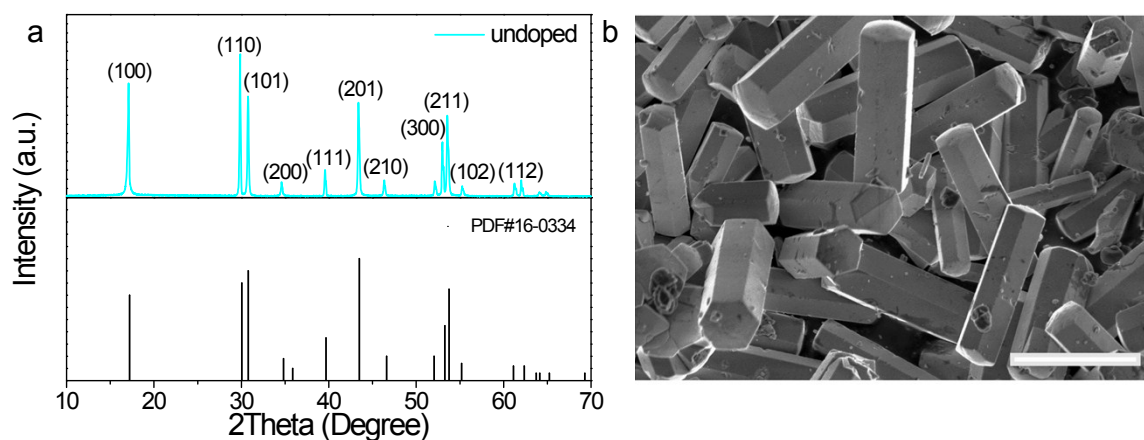


Figure S1. (a) XRD patterns of pure β - NaYF_4 compared to the known peaks of the hexagonal phase of NaYF_4 . (b) SEM images of pure β - NaYF_4 . Scale bars are 10 μm .

The diffraction peaks of undoped β - NaYF_4 can be indexed to the standard data of the hexagonal-phase NaYF_4 (JCPDS 16-0334), confirming that the microcrystals crystallized into a hexagonal host lattice. The morphological characteristic of the sample was in the shape of hexagonal rod.

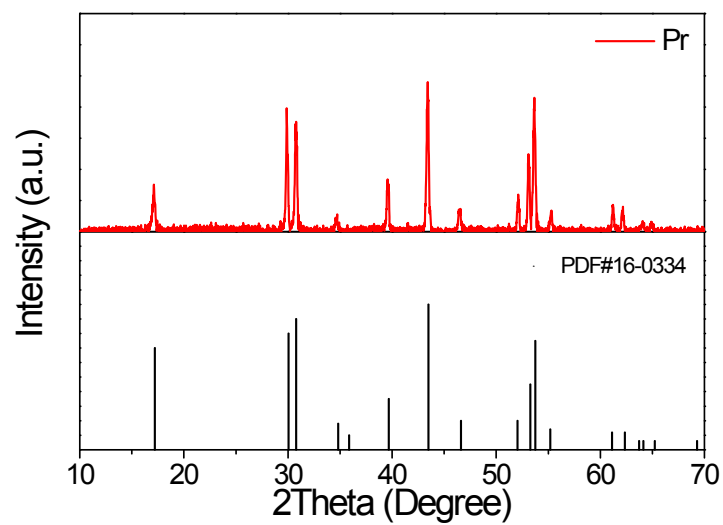


Figure S2. XRD patterns of Pr³⁺ ion single-doped β-NaYF₄.

The diffraction peaks of Pr³⁺ ion single-doped β-NaYF₄ can be indexed to the standard data of the hexagonal-phase NaYF₄ (JCPDS 16-0334), indicating that the doping of Pr³⁺ ions did not change the hexagonal phase structure of the matrix.

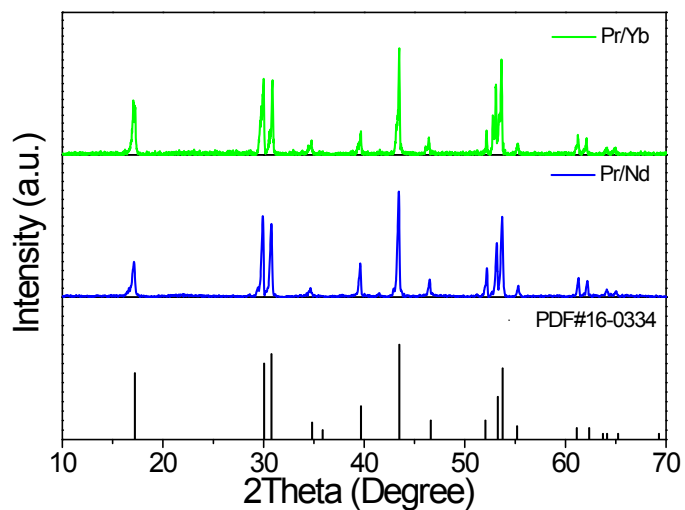


Figure S3. XRD patterns of β -NaYF₄ doped with Pr/Yb, and Pr/Nd compared to the known peaks of the hexagonal phase of NaYF₄.

The diffraction peaks of rare earth ions double-doped β -NaYF₄ can be indexed to the standard data of the hexagonal-phase NaYF₄ (JCPDS 16-0334), which were strong and sharp, indicating that the samples were highly crystalline.

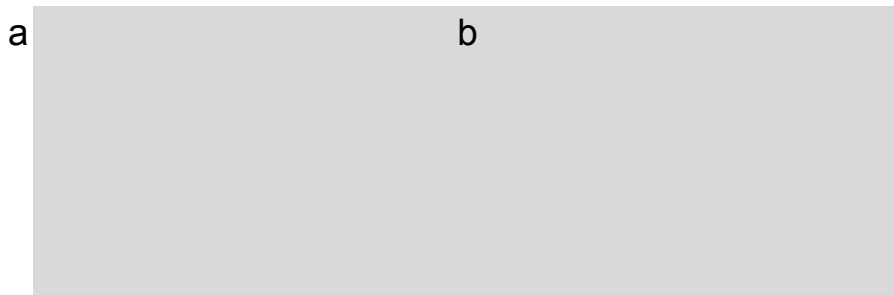


Figure S4. SEM images of β -NaYF₄ doped with (a) Pr/Yb, and (b) Pr/Nd. Scale bars are 10 μ m.

The particles show uniform size and morphology according to the SEM images. The morphological characteristics of the samples were all in the shape of hexagonal rod, which the microrods were around ~ 2.5 μ m in diameter and ~ 10 μ m in length.

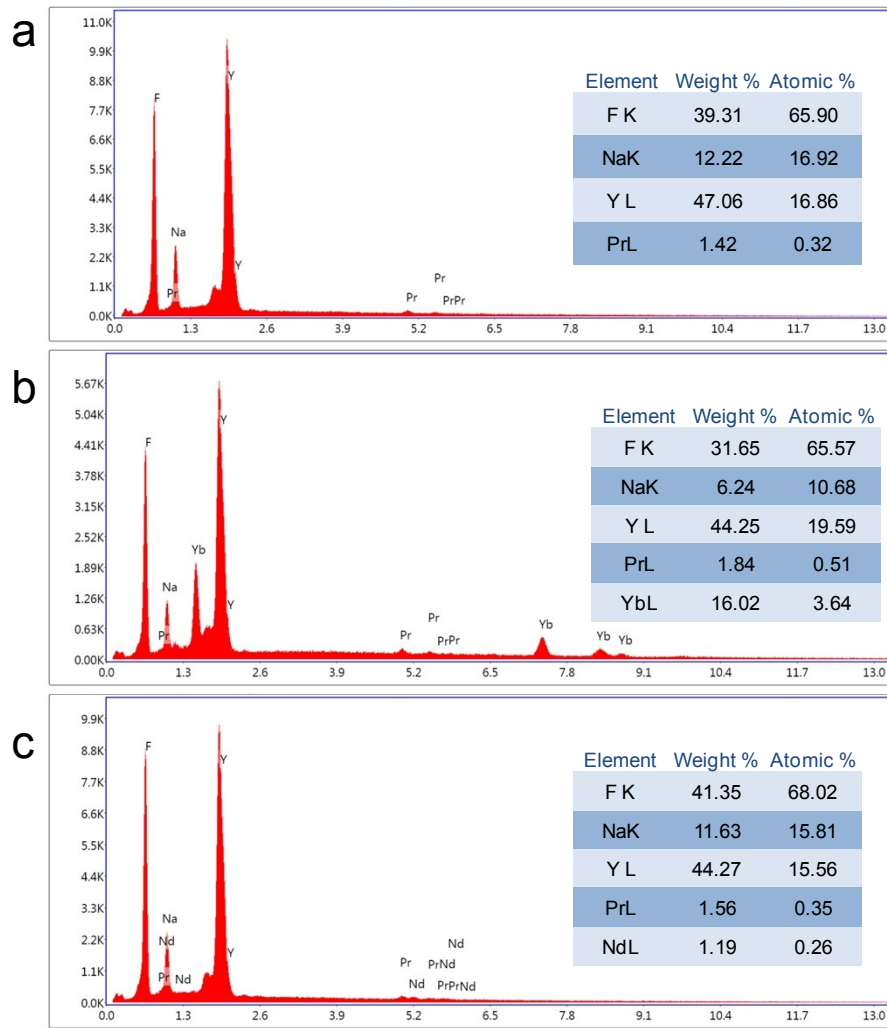


Figure S5. Energy-Dispersive X-Ray Spectroscopy (EDS) of (a) Pr, (d) Pr/Nd, and (f) Pr/Yb samples.

The content of the doped rare earth element can be confirmed by compositional analysis. In the Pr-doped sample, the content percentage of the rare earth element (Y:Pr) is 98.14%: 1.86%, the percentage of Y:Yb:Pr is 82.52%: 15.33%: 2.15% in the Pr/Yb-doped sample, and the percentage of Y:Nd:Pr is 96.23%: 1.61%: 2.16% in Pr/Nd doped samples.

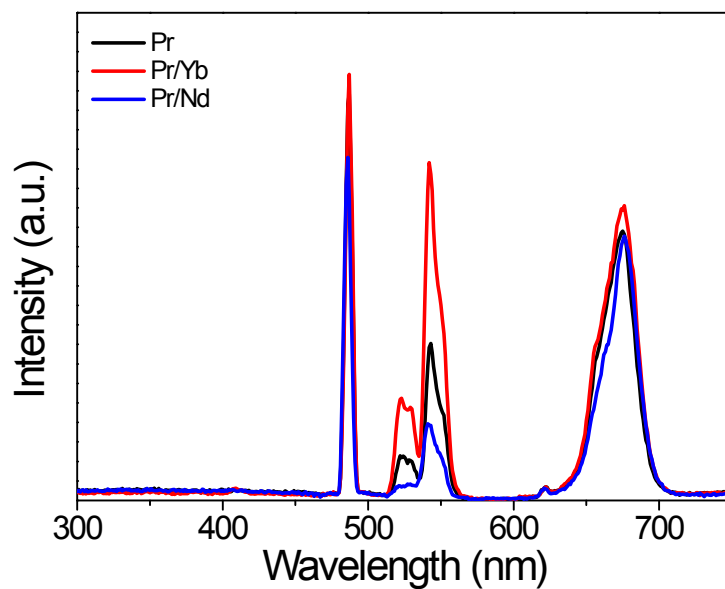


Figure S6. UC emission spectra of $\text{NaYF}_4:\text{Pr}^{3+}$, $\text{NaYF}_4:\text{Pr}^{3+}/\text{Yb}^{3+}$, and $\text{NaYF}_4:\text{Pr}^{3+}/\text{Nd}^{3+}$ samples under 980 nm laser excitation ($29.8 \text{ mW}/\text{mm}^2$).

The effect of the addition of different rare earth ions on the UC luminescence properties of Pr^{3+} doped materials were investigated under the same excitation conditions. It was found that the UC luminescence intensity of the Pr^{3+} doped material increases when Yb^{3+} is co-doped, while the green luminescence intensity decreases when Nd^{3+} is co-doped.

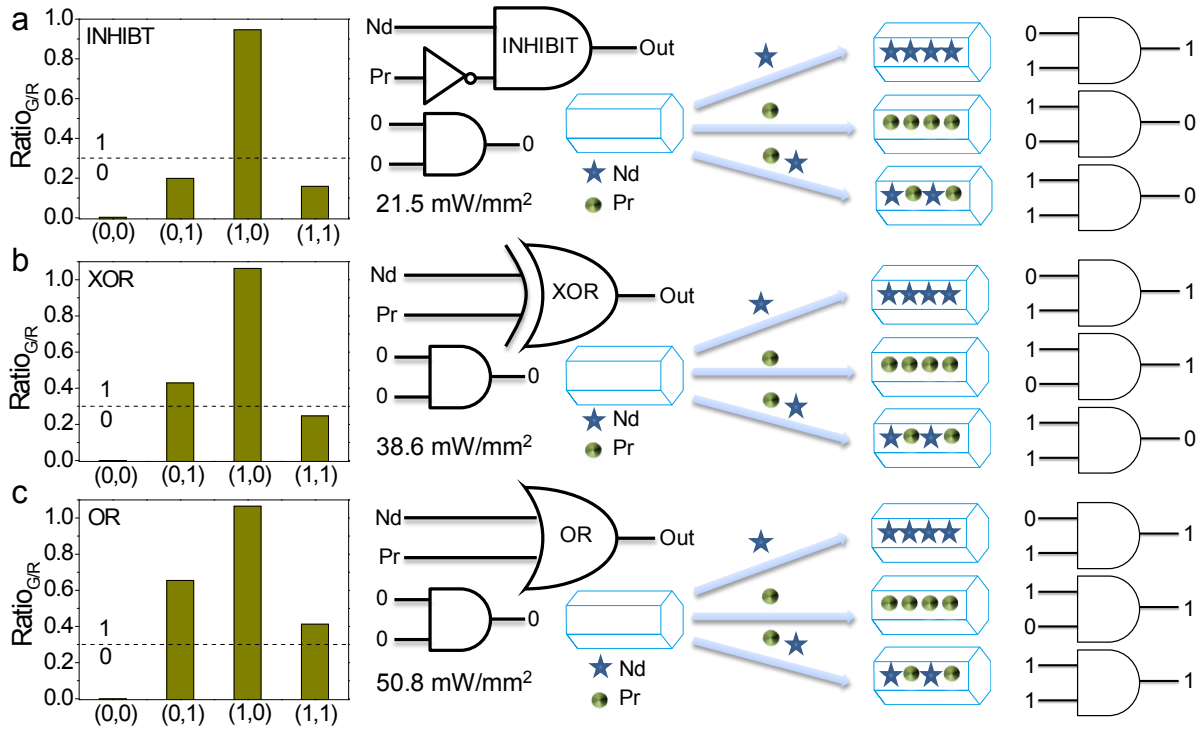


Figure S7. Schematic illustrations of the fabrication procedures of UC (a) INHIBIT, (b) XOR, and (c) OR logic gates under different excitation power density.

The logic operations such as INHIBIT, OR, and XOR gates are the basic units of logic circuits, which perform "INHIBIT", "OR", and "XOR" logical operations, respectively. In the logic gate operation, the INHIBIT gate can be expressed as: when only the input signal Input (A) does not exist and Input (B) exists, the output is "1", and the output is "0" in other cases. The operation of XOR logic operation is that when the two signal inputs are different, the output signal is "1"; when the two input signals are the same, for example, if both input signals are "0" or both input signals are "1", then the output signal is "0". The logical function performed by the "OR" gate is

that when an input signal is true, the output result is true, and the output is false only when all input signals are false. The logic gates could be constructed by utilizing these UC materials. We can control the green/red emission ratio of the UC materials by the excitation power modulation method, which could implement the corresponding logic operations. Herein, rare earth ions Nd^{3+} and Pr^{3+} acted as the two inputs signals and the green-red ratio could be regarded as the output signals. By defining an intensity threshold to separate ON and OFF states among the UC green-red ratio values, we could achieve the construction of logic operations with two input terminals and one output terminal. The output below and above the threshold value of 0.3 are defined as “0” and “1”, respectively.

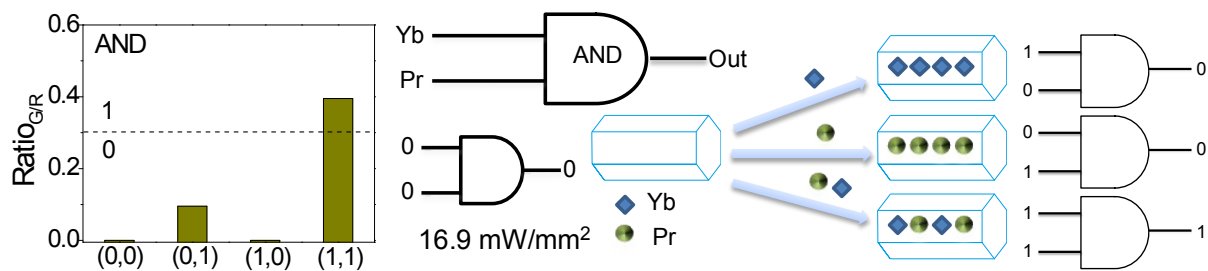


Figure S8. Schematic of the UC luminescence system which performs the AND logic gate under the action of Yb³⁺ and Pr³⁺ inputs. The dashed line shows the threshold that separates output 0 and 1.

It is also possible to build another logic gates by changing the input conditions. When the input conditions are Yb³⁺ and Pr³⁺, an AND logic gate could be constructed under the excitation power density of 16.9 mW mm⁻². In the presence of either inputs (1/0, 0/1), a true output of “0” is obtained, while in the presence of both Yb³⁺ and Pr³⁺, the resulting green-red ratio is higher than 0.3 and the output signal was “1”.

Table S1. Lattice parameters and crystal volume of the systems.

System	$a=b/\text{nm}$	c/nm	V/nm^3	$\alpha/^\circ$	$\beta/^\circ$	$\gamma/^\circ$
$\beta\text{-NaYF}_4$	1.164	0.688	0.808	90	90	120
$\beta\text{-NaYF}_4\text{:Pr}$	1.174	0.694	0.828	90	90	120

All of the lattice structures retain their original hexagonal structures, that is, $\alpha = \beta = 90^\circ$ and $\gamma = 120^\circ$, without significant structure distortion. The doped lattice parameters and crystal volume did not change much compared to undoped system, indicating that the results are credible.

Table S2. Cohesive energy of the systems.

System	β -NaYF ₄	β -NaYF ₄ :Pr
The cohesive energy (eV/atom)	-5.65	-5.55

Cohesive energy is usually negative, and the smaller the value is, the more stable the substance is.

The absolute value of the cohesive energy of the doped system is reduced, indicating that the stability of the doping system is lower than that of the undoped system, but the small decrease does not affect the doping system in a stable state.

Table S3. Color coordinates of the NaYF₄:Pr at different excitation powers.

Pump power (mw/mm ²)	x	y
2.0	0.51	0.3045
4.0	0.4916	0.3029
8.2	0.4199	0.3178
16.9	0.3202	0.3529
21.5	0.3046	0.3778
29.8	0.282	0.4364
43.0	0.2714	0.4782
58.6	0.2561	0.5321
70.8	0.2597	0.588

Table S4. Color coordinates of the NaYF₄:Pr/Yb sample at different excitation powers.

Pump power (mw/mm ²)	x	y
2.0	0.5299	0.3182
4.0	0.4412	0.3618
8.2	0.3643	0.4034
16.9	0.3285	0.4475
21.5	0.2886	0.5029
29.8	0.2748	0.5331
43.0	0.2656	0.5466
58.6	0.2583	0.5803
70.8	0.2556	0.5935

Table S5. Color coordinates of the NaYF₄:Pr/Nd sample at different excitation powers.

Pump power (mw/mm ²)	x	y
2.0	0.4947	0.2730
4.0	0.4505	0.2721
8.2	0.3869	0.2798
16.9	0.3245	0.3091
21.5	0.2901	0.3439
29.8	0.2822	0.3538
43.0	0.2587	0.4449
58.6	0.2489	0.4835
70.8	0.253	0.5383